N89-24543

Center for Turbulence Research
Proceedings of the Summer Program 1988

Dynamics of coherent structures in a plane mixing layer

By F. Hussain[1], R. Moser[2], T. Colonius[3], P. Moin[2,3] AND M. M. Rogers[2]

An incompressible, time-developing three-dimensional mixing layer with idealized initial conditions has been simulated numerically. Consistent with the suggestions from experimental measurements, the braid region between the dominant spanwise vortices or rolls develops longitudinal vortices or ribs, which are aligned upstream and downstream of a roll and produce spanwise distortion of the rolls. The process by which this distortion occurs has been explained by studying a variety of quantities of dynamic importance (*e.g.* production of enstrophy, vortex stretching). Other quantities of interest (dissipation, helicity density) have also been computed and are discussed. The currently available simulation only allows the study of the early evolution (before pairing) of the mixing layer. New simulations in progress will relieve this restriction.

Introduction

While there is no doubt about the occurrence of large-scale coherent structures in turbulent shear flows, there is doubt about their role and dynamical significance. Unfortunately, a mathematical definition of coherent structures or a theory of turbulence based on coherent structures has not yet been developed, nor is there any in sight. Until the development of a theoretical framework , or even to formulate one, we must continue to improve our understanding of coherent structures. Studies of coherent structures in shear flows, in particular the mixing layer, have focused on the geometric form of the structures (morphology) and the relationship of the structures to topological features of the flow (*e.g.* the stagnation line and saddle between rolls in the mixing layer); also of interest are quantitative measures of dynamical quantities such as coherent Reynolds stress and coherent production. Experimental observations of coherent structures in the mixing layer have relied on flow visualization techniques (which suffer from the indirect relationship of flow markers to the hydrodynamics) and quantitative point-wise measurements (which are unable to measure the full three-dimensional flow field). Such measurements strongly suggest the complex morphology of the coherent structures in mixing layers, in particular the counter-rotating longitudinal vortices (ribs) in the braid region between the rolls (Bernal & Roshko, 1986, Hussain, 1983). However, the details of these structures are not currently accessible from experimental data. Fortunately,

1 University of Houston
2 NASA Ames Research Center
3 Stanford University

PRECEDING PAGE BLANK NOT FILMED

direct numerical simulation of turbulent flows can provide the 3D flow field with adequate resolution, albeit at low Re (Metcalf *et al.*, 1987, Hussain 1986).

Several numerical simulations were performed to study the details of the coherent structures observed experimentally in mixing layers. A three-dimensional time-developing mixing layer with prescribed initial conditions was simulated. The initial conditions were chosen to produce structures similar to those observed experimentally. These simulations are different from the experiments they are meant to mimic in several important ways. First, the experimental flows are spatially developing, whereas the simulations are time developing. The time-developing simulation approximates the evolution of a structure in the spatially-developing flow as it travels downstream. Second the initial conditions do not necessarily reflect the conditions present in an experiment. In the simulations the initial conditions are very smooth and simple, there is no small-scale random motion, thus the resulting flow fields are not turbulent. These simple conditions are used so that the coherent structures can be studied in their simplest form. The question of how the observed structures evolve from conditions actually present in experiments, and how they respond to small-scale random disturbances is left to future work. Finally, the Reynolds number in the simulations is quite low compared to experiments.

The simulations were performed using a numerical method similar to that discussed by Cain, Ferziger & Reynolds (1984). In this method periodic boundary conditions are applied in the streamwise (x) and spanwise (z) directions, and Fourier series are used in these directions. An infinite domain in the cross-stream direction (y) is treated by using a coordinate transformation which maps the domain into a finite interval. Fourier series are then used in the finite interval. In the particular simulation to be discussed below, 32 Fourier modes were used in the x and z directions and 64 modes were used in the y direction. The length of the computational domain in the x direction was $4.48\pi\delta$, and in the z direction it was $2.7\pi\delta$ where δ is the initial vorticity thickness of the layer. The initial velocity field consisted of an error function velocity profile and a pair of three-dimensional disturbances. The first disturbance leads to the two-dimensional Kelvin-Helmholtz roll-up of the mixing layer and ultimately pairing, the initial spanwise vorticity in this disturbance is given by

$$\omega_z = 0.1 f_1(y)\cos(\frac{x}{1.12\delta}) + 0.05 f_2(y)\cos(\frac{x}{2.24\delta}).$$

where the functions f_1 and f_2 are Rayleigh eigenfunctions and the wave-lengths are chosen to be the most unstable and its subharmonic. The second disturbance leads to the longitudinal vortices in the braid region between the Kelvin-Helmholtz rolls. This disturbance initially consists of an array of streamwise vortices described by

$$\omega_x = 0.05 g_1(y) sin(\frac{z}{0.675\delta}) + 0.025 g_2(y) sin(\frac{z}{1.35\delta})$$

where the functions g_1 and g_2 were chosen to represent streamwise vortices and the wave-lengths were chosen to be the most unstable and its subharmonic. A Reynolds number of 1000 based on initial vorticity thickness and velocity difference was used in this simulation.

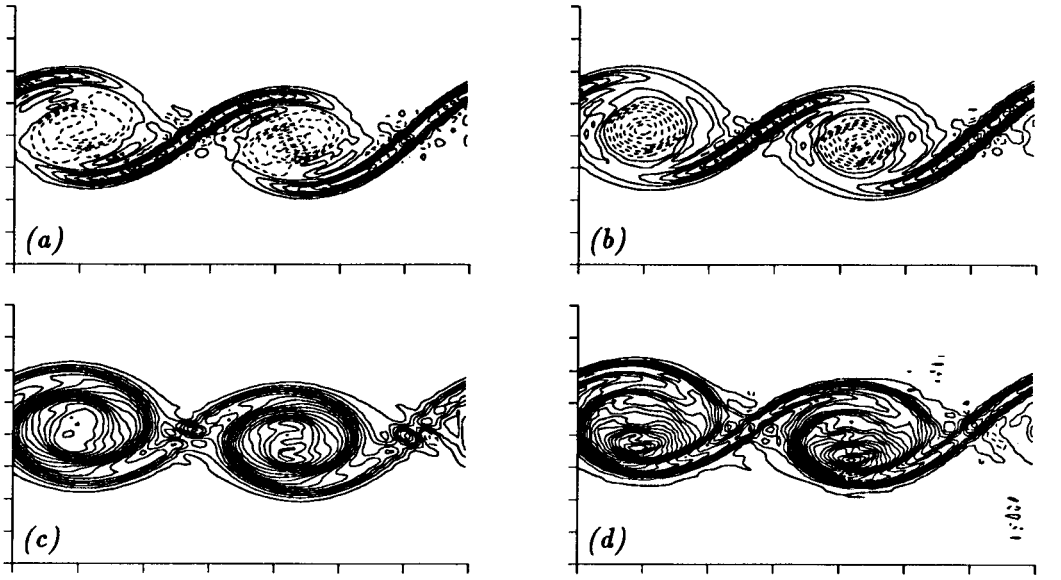

FIGURE 1. Vorticity contours in plane 1; (a), ω_x, (b), ω_y and (c), ω_z, and plane 2; (d), ω_z at time I. Contour increment is $0.1U/\delta$. Negative contours are dashed in $(a)$and (b), positive contours are dashed in $(c)$and (d). Streamwise (x) direction is horizontal; cross stream (y) direction is vertical.

Results and Discussion

For the current discussion we have selected two instants in the simulation described above: time I ($t = 26.4\delta/\Delta U$) is when the initial Kelvin-Helmholtz roll-up is saturating and the two rolls are nearly identical, and time II ($t = 35\delta/\Delta U$) is a short time later when the pairing interaction has started. To study the pairing process, a much later time is required; however, the current simulation was stopped at $t = 17.5$ because of lack of resolution. Higher resolution simulations are being performed to address questions of pairing. In the discussion to follow, two dimensional contour plots of various quantities will be presented in two planes in the flow field. The first plane (plane 1) is an x-y plane (plane of constant z) which passes through the center of the longitudinal vortices (location of maximum streamwise vorticity). The second plane (plane 2) is also an x-y plane, and it passes halfway between the longitudinal vortices (streamwise vorticity is zero in this plane).

Contours of the three components of vorticity in both planes at time I are shown in figure 1 (ω_x and ω_y are identically zero in plane 2). The role-up of the shear-layer resulting in the concentration of spanwise vorticity in two large rolls is clearly evident. Note that there is substantial spanwise vorticity in the braid region between the rolls (as much as -0.55) compared to the initial maximum spanwise vorticity (-2) As the roll-up continues, spanwise vorticity continues to be swept from the braid region; at time II (figure 2) the spanwise vorticity in the braid region has been reduced to -0.25. The streamwise and cross-stream vorticity (ω_x and ω_y in figures $1(a,b)$ are concentrated in the braid region as expected; these are the longitudinal

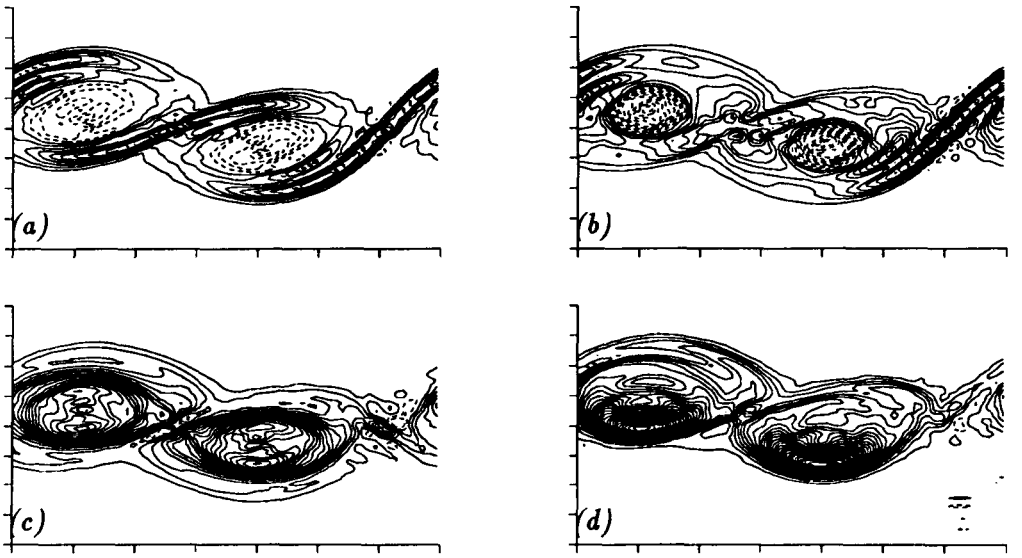

FIGURE 2. Vorticity contours in plane 1; (*a*), ω_x, (*b*), ω_y and (*c*), ω_z, and plane 2; (*d*), ω_z at time II. Contour increment is (*a*), $0.15U/\delta$, (*b,c,d*), $0.1U/\delta$. Negative contours are dashed in (*a*)and (*b*), positive contours are dashed in (*c*)and (*d*). Streamwise (x) direction is horizontal; cross stream (y) direction is vertical.

(or rib) vortices. They include both ω_x and ω_y because they are inclined. There are, of course, an array of counter-rotating rib vortices, the ones in this plane have positive vorticity but in other planes the vorticity would be negative. The rib vortices lie along the diverging separatrix of the stagnation point between the two main rolls. Therefore they are subjected to a plane strain which stretches them along the separatrix. The result is an increase in the vorticity magnitude with time ($\omega_x = 0.65$ at time I, and 0.98 at time II, see figures 1 and 2).

In the rolls there is a somewhat weaker region of streamwise and cross-stream vorticity of opposite sign to that in the ribs ($\omega_x = -0.35$ at time I). This is apparently a result of the three-dimensional distortion of the rolls by the ribs. This distortion is most apparent at time II where there is a marked difference in the spanwise vorticity contours in planes 1 and 2 (figures 2(*c,d*)). In plane 2, the spanwise vorticity is concentrated near the bottom of the rolls and is very strong there (-3.05) compared to the initial maximum spanwise vorticity (-2.0). In plane 1, the vorticity is more evenly distributed through the roll and has a maximum value of -1.85. The mechanism by which the ribs produce three-dimensionality in the rolls can be understood by examining the rate of production of enstrophy ($\omega_i S_{ij} \omega_j$, where $S_{ij} = \frac{1}{2}(\partial u_i/\partial x_j + \partial u_j/\partial x_i)$) at time II (figure 3). In plane 2 there is a region of strong enstrophy production coinciding with the concentrated region of spanwise vorticity. Above it there is also a region of negative enstrophy production. The strong production is a consequence of the stretching of the spanwise vorticity. This stretching occurs in the region between the counter-rotating rib vortices where

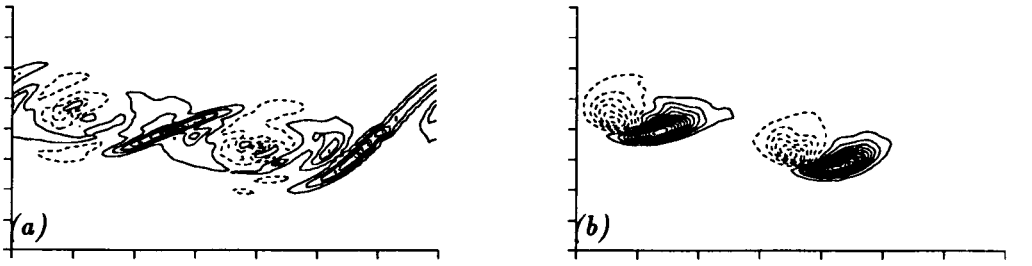

FIGURE 3. Rate of enstrophy production in (a), plane 1 and (b), plane 2 at time II. Contour increment is $0.2U^3/\delta^3$. Negative contours are dashed. Streamwise (x) direction is horizontal; cross stream (y) direction is vertical.

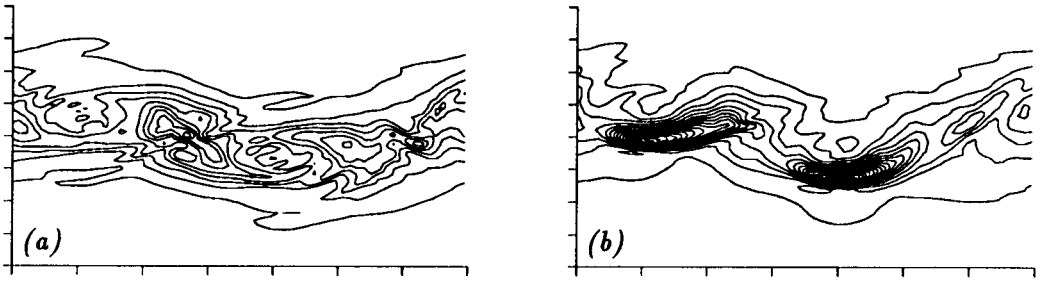

FIGURE 4. Dissipation of kinetic energy in (a) plane 1 and (b) plane 2 at time II. Contour increment is $0.0005U^3/\delta$. Streamwise (x) direction is horizontal; cross stream (y) direction is vertical.

the strain $\partial w/\partial z$ is large and negative. Between rib vortices where $\partial w/\partial z$ is positive compression occurs resulting in the negative enstrophy production mentioned above. In plane 1, which is through the center of the rib vortices ($\partial w/\partial z = 0$), the enstrophy production in the rolls is small. There is however enstrophy production in the braid region, corresponding to the stretching of the rib vortices.

Another quantity of interest is the dissipation of kinetic energy, which is shown at time II in figure 4. The dissipation is rather weak in plane 1 (0.003) compared to plane 2 (0.009). In particular, the dissipation in plane 2 is concentrated in the region of large ω_z and large enstrophy production discussed in the previous paragraph. Thus the three dimensional distortion of the rolls results in significant dissipation of kinetic energy. The work of Moffatt (1985) on inviscid flows suggests that dissipation and helicity density ($u_i\omega_i$) should be spatially exclusive; however, Hussain (1986) suggests that this may not be the case. Helicity density and dissipation contours in plane 1 at time I are shown in figure 5. Helicity density is identically zero in plane 2. The helicity density is concentrated in the region where the ribs meet the rolls and is zero near the stagnation point between the rolls; this is as suggested by Hussain (1986). We note that there is also a concentration of dissipation in the braid region, thus at this time the dissipation and helicity density are not spatially exclusive. This may be a consequence of low Reynolds number or the early stage of

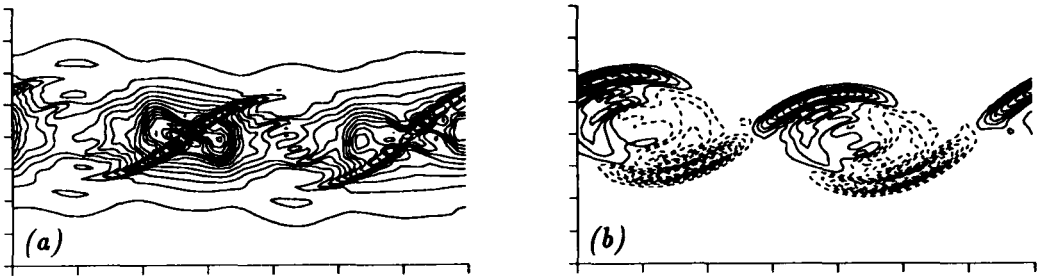

FIGURE 5. Dissipation of kinetic energy (a) and helicity density (b) in plane 1 at time I. Contour increment is (a), $0.00025U^3/\delta$ and (b), $0.1U^2/\delta$. Negative contours are dashed. Streamwise (x) direction is horizontal; cross stream (y) direction is vertical.

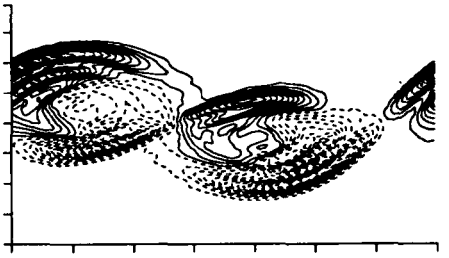

FIGURE 6. Helicity density in plane 1 at time II. Contour increment is $0.1U^2/\delta$. Streamwise (x) direction is horizontal; cross stream (y) direction is vertical.

development of the flow. At time II the dissipation is not significantly concentrated in the braid region (see figure 4), whereas the helicity density is nearly the same as the earlier time (figure 6). Thus at time II the peak of dissipation occurs in plane 2, where the helicity density is zero, and the peak of the helicity density occurs in plane 1 where the dissipation is minimum.

Summary

A simulation of a time-developing mixing layer with idealized initial conditions has produced flow structures which are at least qualitatively similar to those observed in experimental mixing layers. With the availability of the three-dimensional flow field, it is possible to investigate a variety of structural and dynamical questions by computing any number of flow quantities (*e.g.* vorticity, production of enstrophy, dissipation etc.). For example, in this brief study we were able to observe and explain the three-dimensional distortion of the Kelvin-Helmholtz rolls by the rib vortices, and we were able to study the relationship of helicity density and dissipation. A more complete study of higher-resolution simulations should provide great insight into the dynamics and topology of coherent structures in the mixing layer. This is the focus of our ongoing research.

REFERENCES

BERNAL, L. P. & ROSHKO, A. 1986 Streamwise vortex structure in plane mixing layers. *J. Fluid Mech.* **170**, 499-525.

CAIN, A. B., FERZIGER, J. H. & REYNOLDS, W. C. 1984 Discrete orthogonal function for non-uniform grids using the fast Fourier transform. *J. Comp. Phys.* **56**, 272-286.

HUSSAIN, A. K. M. F. 1983 *Turbulence and Chaotic Phenomena in Fluids* (ed. T. Tatsumi), p.453.

HUSSAIN, A. K. M. F. 1986 Coherent structures and turbulence. *J. Fluid Mech.* **173**, 303-356.

MOFFATT, H. K. 1985 Magnetostatic equilibria and analogous Euler flows of arbitrarily complex topology. Part 1. Fundamentals. *J. Fluid Mech.* **159**, 359-378.

METCALF, R. W., ORSZAG, S. A., BRACHET, M. E., MENON, S. & RILEY, J. J. 1987 Secondary instability of temporally growing mixing layer. *J. Fluid Mech.* **184**, 207-243.

Page intentionally left blank